Energy Harvesting Enabled Full-Duplex Cooperative Relaying System over Fisher-Snedecor F-Distribution Fading Channel

Kehinde O. Odeyemi and Pius A. Owolawi
Department of Computer Systems Engineering, Tshwane University of Technology, Pretoria-0001, South Africa
Email: kesonics@yahoo.com; p.owolawi@gmail.com

***Abstract*—**In this paper, the performance of an Energy Harvesting (EH) enabled full-duplex cooperative decode-and-forward (DF) relaying system is investigated over the Fisher-*Snedecor* F-fading channel. The system energy-constrained relay unit utilizes time-switching relay protocol for scavenging energy from the source signal and information transmission to the destination. To quantify the system performance, the exact analytical closed-form expression for the system outage probability is derived, and then used to obtain the analytical expression for the average throughput of delay-limited transmission mode. Moreover, the exact closed-form expression for the system Ergodic capacity is derived through which the average delay-tolerant throughput is determined for the system. In addition, the results demonstrate the impact of fading and shadowing severity on the system performance. It also is noticeable from the results that the performance of system is strongly affected by the loop back interference from the relay node. Finally, the accuracy of the derived analytical expressions is then validated through the Monte-Carlo simulation.

***Index Terms*—**Full-duplex, Energy harvesting, Fisher-Snedecor fading, decode-and-forward relaying

I. Introduction

A. Information Background

Cooperative relaying technology has been considered as an effective technique of improving the performance of wireless communication systems while extending the its coverage area most especially, in strongly-shadowed environment [1]. In designing of relaying systems, the selection between the Full-Duplex (FD) and Half-Duplex (HD) relaying mode is one of the vital factors to be considered. Thus, in conventional relaying system, where the operation is in Half-Duplex (HD) mode, the relay node receive and transmit source signal to the destination in orthogonal time slots [2]. This operation mode is simple to design and implement, but leads to significant reduction in the system spectral efficiency. As a result of this, full-duplex relaying technique have attracted a lot of attention in research community due to ultimate usage of radio resources [3]. Comparing to HD relaying systems, the relay has capability to receive and transmit source signal simultaneously on the same frequency band to achieve higher spectral efficiency [4].

However, the issues of residual self-interference between the relay transmit and receive antenna severely limit the system performance [5]. Thus, with various development of self-interference cancellations and hardware designs, FD operation mode has been suggested as a potential enabling technique for improving the throughput performance of fifth generation (5G) wireless systems over existing HD mode [6]-[8]. The FD relaying system can be classified into Amplify-and-Forward (AF) relaying systems and Decode-and-Forward (DF) relaying systems [9]. The AF relay received and amplifies the source signal with the inclusion of desired signal, noise, self-interference to the destination. On the other hand, the DF relay firstly decode the source signal and transmit the re-encode signal to the destination. Therefore, the residual self-interference does not affect the relay to destination link [7].

Wireless energy transfer has been emerged as a promising solution in energy-constrained wireless networks where it is impossible to replace or recharge the batteries of wireless devices [10]. This technique allows the wireless devices to harvest energy from any external natural resources such as solar, wind or vibration. However, the amount of energy that can be harvested from these natural resources is unpredictable due to the uncontrollable factors such as weather conditions that make the communication reliability highly difficult [11]. To overcome this challenge, harvesting energy through Radio Frequency (RF) have been suggested for wireless devices due to its capability to carry both information and energy simultaneously [12]. Practically, this could be realized through the Time-Switching Relaying (TSR) and Power-Splitting Relaying (PSR) protocols. In TSR protocol, there is division of transmission time frame into two parts with one used to harvest energy from the source while the remaining is designate for information transmission. On the other hand, in PSR protocol, the transmission time is evenly divided for the receive node to harvest energy and information processing [13]. Therefore, to prolong the lifetime of a full-duplex relaying systems, there is need to combine EH technique in which the relay nodes scavenge energy from the source signal and utilizes it to forward the intended information to a corresponding destination.

Manuscript received August 2, 2020; revised February 7, 2021.
doi:10.12720/jcm.16.3.82-90

©2021 Journal of Communications

B. Related Works and Motivation

Scanning through the open literature, it was found that the performance of FD relaying system in the context of energy harvesting has been extensively studied under different fading distributions environment/channel. The authors in [11] investigated the performance of a dual-hop FD relaying system under AF and DF relaying protocols. A wireless powered full-duplex DF-based multiple input multiple output relaying system was studied in [6] where the performance of interference mitigation schemes were evaluated. In [8], the performance of a FD-DF relaying system with EH was analysed in terms of outage probability and symbol error probability. The security performance of a wireless powered FD and HD relaying system was investigated in [14] under the presence of an eavesdropper and a jammer. Also, the security performance of a FD relaying EH assisted system was presented in [15] and the authors obtained the exact expression for the connection outage probability, the secrecy outage probability and the transmission outage probability based on which the secrecy throughput. The performance of an underlay cooperative wireless powered cognitive full-duplex relaying system was proposed in [16]. However, all of the aforementioned works considered FD energy harvesting-enabled relay networks over Rayleigh fading distribution channel. Moreover, the outage probability and energy efficiency of an EH aided non-orthogonal multiple access based FD-AF relaying system was presented in [17] over the Nakagami-m fading channel. A FD-DF relay system is studied in [18] over Nakagami-m fading channel. The source and relay nodes harvest energy from the power beacon and the closed-form expression for the system outage probability with symbol error rate were obtained. Also, the performance of non-cooperative and cooperative energy harvesting enabled FD cognitive radio network was evaluated in [19] over Nakagami-m fading channel. In [20], the energy harvest enabled FD-DF system in indoor environment was in presented where the performance of three EH protocols was evaluated over the log-normal distribution channel. Recently, the outage probability of EH-based FD AF and DF relaying system in $\alpha-\mu$ fading environment was presented in [4]. The performance of wireless powered FD-DF based relaying network was evaluated in [21] where the exact expressions for the system ergodic outage probability was derived over the $k-\mu$ fading distribution. Also, *Rabie et al* [22], analysed the performance of a cooperative relaying non-orthogonal multiple access network over *F* composite fading channels. In [23], the device-to-device communication with energy limited DF relay-assisted system over *F*-distribution channel was studied, where the relay node was assumed to operate in half-duplex mode. However, it is worth noting that no research works have studied the performance of an EH assisted full-duplex relaying systems over the Fisher-*Snedecor* F-distribution fading channel.

C. Contributions

Motivated by the above facts, in this paper, the performance of an energy harvesting enabled full-duplex cooperative DF relaying system over the Fisher-*Snedecor* F-distribution fading channel is investigated. The energy-limited relay node of the concerned system relies on the energy harvesting from the signal transmitted by the source through the time-switching relay protocol. The results reveal the impact of system and channel parameters on the performance. The contributions of this paper are detailed as follows:

a) The exact analytical closed-form expression of the system outage probability over the F-fading channel is derived.
b) Also, the analytical closed-form expression of the Ergodic capacity is obtained for the concerned system over the F-fading channel.
c) Through the outage probability and Ergodic capacity, the average throughput under the delay-limited and delay-tolerant transmission modes are respectively derived.
d) Related to [4], [21] and [23], our system analysis is based on the Fisher-*Snedecor* F-distribution and average throughput under different transmission modes are considered.

The rest of this paper is structured as follows. In Section II, the system and channel models are presented. Section III depicts the performance analysis of outage probability, Ergodic capacity and average throughput under different transmission modes. In addition, the numerical results and discussions are presented in Section IV. Finally, the concluding remarks are presented in Section V

II. System and Channel Models

The system model of a full-duplex cooperative relay network with a source (S), a DF-based relay (R) and a destination (D) is illustrated in Fig. 1. The source and the destination are equipped with a single antenna while the relay has two antennas for receiving and transmitting source data. Owing to the severe shadowing and path-loss impairments, there is no direct link between the S and D. The S-to-R, R-to-D and the l loop-back interference (LBI) links are assumed to follow Fisher-Snedecor fading distributions with channel coefficient denoted as: h_1, h_2 and h_3 respectively. The distance between S-to-R and R-to-D is respectively defined as d_1 and d_2 with the corresponding path-loss exponents given as ζ_1 and ζ_2. Therefore, the overall communication between S and D occurs in two-time phases. During the first phase, the DF relay node has no external power supply but scavenge energy from the transmitting signal from the source using the time-switching relay scheme. In this case, the overall time frame T is then divided into three consecutive time slots. The first time slot αT is designated for energy harvesting while each of the remaining time slot $(1-\alpha)T/2$ is dedicated for S-to-R

and R-to-D information transmission with EH time factor defined with $0 \leq \alpha \leq 1$.

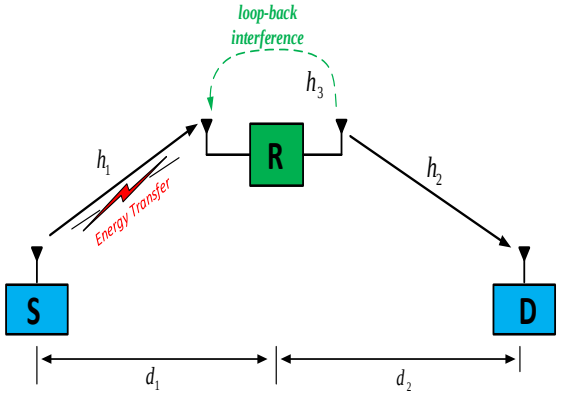

Fig. 1. Full-duplex cooperative relay system model

The received signal at the relay node can then be expressed as:

$$y_R(t) = \sqrt{P_s d_1^{-\zeta_1}} h_1 x(t) + h_3 r(t) + n_R(t) \quad (1)$$

where P_s denotes the source transmit power, $x(t)$ represents the source information signal, r is the LBI signal and the $n_R(t)$ is the Additive white Gaussian noise (AWGN) at the relay node with variance σ_R^2.

As a full-duplex system, the relay node recognises its own signal and it applies interference cancellation to reduce the LBI. Hence, the post-cancellation received signal at relay node can be expressed as:

$$y_R(t) = \sqrt{P_s d_1^{-\zeta_1}} h_1 x(t) + \hat{h}_3 \hat{r}(t) + n_R(t) \quad (2)$$

where $\hat{h}_3$ represents the residual LBI

At the end of the first phase, the total energy harvested by the relay node can be expressed as [21]:

$$E_h = \eta \alpha T \frac{P_s \|h_1\|^2}{d_1^{\zeta_1}} \quad (3)$$

where η denotes the energy conversion efficiency which is mainly affected by the circuitry is given at $0 \leq \eta \leq 1$

During the second transmission phase, the transmit power at the relay node can be computed as:

$$P_R = \frac{E_h}{(1-\alpha)T} = \frac{\xi P_s \|h_1\|^2}{d_1^{\zeta_1}} \quad (4)$$

where $\xi = \frac{\eta\alpha}{1-\alpha}$

Thus, the received signal at the destination can then be written as:

$$y_D(t) = \sqrt{P_R d_2^{-\zeta_2}} h_2 \hat{x}(t) + n_D(t) \quad (5)$$

where $\hat{x}(t)$ is the decoded signal transmit by the relay and $n_D(t)$ denotes the AWGN at the destination with variance σ_D^2.

By utilizing the (2), (4) and (5), the instantaneous signal-to-noise ratio (SNR) at the relay node and destination can be expressed as:

$$\begin{cases} \gamma_R = \dfrac{P_s \|h_1\|^2}{P_R d_1^{\zeta_1} \|h_3\|^2} = \dfrac{1}{\xi \|h_3\|^2} \\ \gamma_D = \dfrac{P_R \|h_2\|^2}{d_2^{\zeta_2} \sigma_D^2} = \dfrac{\xi P_R \|h_1\|^2 \|h_2\|^2}{d_1^{\zeta_1} d_2^{\zeta_2} \sigma_D^2} \end{cases} \quad (6)$$

As earlier mentioned, all the channels within the system are assumed to follow F-fading distribution. This is due to the fact that it can provide better fit for the modelling of channel data compared to generalized K distribution [24]. In this case, the small-scale fading follows the Nakagami-m distribution while the root-mean square (rms) power of the random variation of the mean signal power is shaped by the inverse Nakagami-m distribution. Thus, the probability distribution function (PDF)of F-distribution can be expressed as [25], [26]:

$$f_{\gamma_p}(\gamma_p) = \frac{\psi_p \gamma_p^{m_p - 1}}{(m_p \gamma_p + \lambda_p)^{m_p + m_{s,p}}} \quad (7)$$

where $p \in \{1,2,3\}$ and $\lambda_p = m_{s,p}\Omega_p$. m_i , $m_{s,p}$ and Ω_p denote the fading severity parameter, the amount of shadowing of the root-mean-square (rms) signal power and mean power respectively of $p-th$ link. $\psi_p = {m_p}^{m_p} {\lambda_p}^{m_{s,p}} / B(m_p, m_{s,p})$ with the $B(.,.)$ represents the Beta function and $\psi_p = \frac{{m_p}^{m_p} {\lambda_p}^{m_{s,p}}}{B(m_p, m_{s,p})}$

By integrating (7), the cumulative distribution function (CDF) for the links can be obtained as [27]:

$$F_{\gamma_p}(\gamma_p) = \frac{{m_p}^{m_p - 1} {\gamma_p}^{m_p} \cdot {}_2F_1(m_p + m_{s,p}, m_p, m_p + 1; -m_p\gamma_p/\lambda_p)}{B(m_p, m_{s,p}) {\lambda_p}^{m_p}} \quad (8)$$

where ${}_2F_1(a,b,c;d)$ is the Gauss hypergeometric function. Thus, for easy analysis, the Gauss hypergeometric function in (8) is converted to Meijer-G function by using the identity defined in [28], then the F-distribution CDF can further expressed as:

$$F_{\gamma_p}(\gamma_p) = \Delta_p {\gamma_p}^{m_p+1} G_{2,2}^{1,2}\left(\frac{m_p\gamma_p}{\lambda_p} \middle| \begin{matrix} -(m_p + m_{s,p}), -m_p \\ -1, -(1+m_p) \end{matrix}\right) \quad (9)$$

where $\Delta_p = \frac{\Gamma(m_p+1){m_p}^{m_p}}{\Gamma(m_p+m_{s,p})\Gamma(m_p)B(m_p,m_{s,p}){\lambda_p}^{m_p+1}}$ and $\Gamma(.)$ denotes the Gamma function

III. Performance Analysis

A. Outage Probability

In this section, the exact closed-form expression for the system outage probability is derived. The outage probability can be described as the probability that the

instantaneous capacity of the first and second links fall below a predefined threshold value $R_{th}(bps/Hz)$. Thus, by assuming that $A = \|h_1\|^2$, $B = \|h_2\|^2$, $D = \|h_3\|^2$ and $T = AB$, the system outage probability can be defined as [21]:

$$P_{out} = Pr(min(C_1, C_2) < R_{th}) \triangleq Pr\left(min\left(\frac{1}{\xi D}, \frac{\xi P_s T}{d_1^{\zeta_1} d_2^{\zeta_2} \sigma_D^2}\right) < \omega\right) \quad (10)$$

Since random variable (RV) of D and T are independent, the system outage probability can be further expressed as:

$$P_{out} = 1 - F_D\left(\frac{1}{\xi\mu}\right)\left(1 - F_T(\mu\Theta)\right) \quad (11)$$

where $\mu = 2^{\frac{R_{th}}{1-\alpha}} - 1$ and $\Theta = \frac{d_1^{\zeta_1} d_2^{\zeta_2} \sigma_D^2}{\xi P_S}$

Through the (9), the CDF of RV of D can be determined as:

$$F_D(\mu) = \frac{\Delta_3}{\xi^{m_3+1}} \mu^{-(m_3+1)} G_{2,2}^{1,2}\left(\frac{m_3}{\lambda_3 \mu \xi}\middle| \begin{matrix} -(m_3 + m_{s,3}), -m_3 \\ -1, -(1+m_3) \end{matrix}\right) \quad (12)$$

Moreover, the CDF of RV of T can be obtained as:

$$F_T(g) = \int_0^\infty F_A\left(\frac{g}{\omega}\right) f_B(\omega) d\omega \quad (13)$$

By using (7) as the PDF of the RV $B$and utilizing (9) as CDF of RV A in (13), the CDF of RV of T can be expressed as:

$$F_T(g) = \psi_2 \Delta_1 g^{m_1+1} \int_0^\infty \omega^{m_2-m_1-2} (m_2 \nu + \lambda_2)^{-(m_2+m_{s,2})} \times G_{2,2}^{1,2}\left(\frac{m_1 g}{\lambda_1 \omega}\middle| \begin{matrix} -(m_1 + m_{s,1}), -m_1 \\ -1, -(1+m_1) \end{matrix}\right) d\omega \quad (14)$$

By simple variable transformation, the (14) can be further be expressed as:

$$F_T(g) = \frac{\psi_2 \Delta_1 g^{m_1+1}}{{m_2}^{m_2-m_1-1}} \int_0^\infty k^{(m_2-m_1-1)-1} (k + \lambda_2)^{-(m_2+m_{s,2})} \times G_{2,2}^{1,2}\left(\frac{m_1 m_2 g}{\lambda_1 k}\middle| \begin{matrix} -(m_1 + m_{s,1}), -m_1 \\ -1, -(1+m_1) \end{matrix}\right) dk \quad (15)$$

By inverting the Meijer-G function using the identity detailed in [28, Eq.(9.31(2))] and apply the integral identity defined in [28, Eq.(7.811(5))], (15) can be solved as it is given in (16) with $\varphi = m_2 + m_{s,2}$ and $\rho = m_2 - m_1 - 1$

$$F_T(g) = \frac{\psi_2 \Delta_1 {\lambda_2}^{\rho-\varphi}}{{m_2}^\rho \Gamma(\varphi)} g^{m_1+1} G_{3,3}^{3,2}\left(\frac{\lambda_1 \lambda_2}{m_1 m_2 g}\middle| \begin{matrix} 1-\rho, 2, (2+m_1) \\ \varphi - \rho, (1 + m_1 + m_{s,1}), (1+m_1) \end{matrix}\right) \quad (16)$$

$$P_{out} = 1 - \frac{\Delta_3}{\xi^{m_3+1}} \mu^{-(m_3+1)} G_{2,2}^{1,2}\left(\frac{m_3}{\lambda_3 \mu \xi}\middle| \begin{matrix} -(m_3 + m_{s,3}), -m_3 \\ -1, -(1+m_3) \end{matrix}\right) + \frac{\psi_2 \Delta_1 \Delta_3 {\lambda_2}^{\rho-\varphi} \Theta^{m_1+1}}{{m_2}^\rho \Gamma(\varphi) \xi^{m_3+1}} \times \mu^{m_1-m_3} G_{2,2}^{1,2}\left(\frac{m_3}{\lambda_3 \mu \xi}\middle| \begin{matrix} -(m_3 + m_{s,3}), -m_3 \\ -1, -(1+m_3) \end{matrix}\right) G_{3,3}^{3,2}\left(\frac{\lambda_1 \lambda_2}{m_1 m_2 \Theta \mu}\middle| \begin{matrix} 1-\rho, 2, (2+m_1) \\ \varphi - \rho, (1 + m_1 + m_{s,1}), (1+m_1) \end{matrix}\right) \quad (17)$$

Thus, the outage probability can be obtained as it is expressed in (17).

B. Ergodic Capacity

The Ergodic capacity can be defined as the mutual information per unit bandwidth and can be expresses as in terms of complementary CDF (CCDF) as follows [29], [30]:

$$\bar{C} = \frac{1}{ln(2)} \int_0^\infty (1+\gamma)^{-1} F_\gamma^c(\gamma) d\gamma \quad (18)$$

where $F_\gamma^c(\gamma)$ is the CCDF

By putting (17) into (18), the Ergodic capacity for the under studied system can be expressed as:

$$\bar{C} = \beth_1 - \beth_2 \quad (19)$$

where

$$\beth_1 = \frac{\Delta_3}{ln(2) \xi^{m_3+1}} \int_0^\infty \mu^{-(m_3+1)} (1+\mu)^{-1} \times G_{2,2}^{1,2}\left(\frac{m_3}{\lambda_3 \mu \xi}\middle| \begin{matrix} -(m_3 + m_{s,3}), -m_3 \\ -1, -(1+m_3) \end{matrix}\right) d\mu \quad (20)$$

By inverting the Meijer-G function using the identity defined in [28, Eq.(9.31(2))] and applying the integral identity detailed in [28, Eq.(7.811(5))], the first term of (19) can be obtained as:

$$\beth_1 = \frac{\Delta_3}{ln(2) \xi^{m_3+1}} G_1 \quad (21)$$

where $G_1 = G_{3,3}^{3,2}\left(\frac{\lambda_3 \xi}{m_3}\middle| \begin{matrix} 1+m_3, & 2, & 2+m_3 \\ 1+m_3, & 1+m_3+m_{s,3}, & 1+m_3 \end{matrix}\right)$

Then,

$$\mathfrak{I}_2 = \frac{\Xi}{ln(2)} \int_0^{\infty} \mu^{m_1-m_3}(1+\mu)^{-1} \times G_{2,2}^{1,2}\left(\frac{m_3}{\lambda_3\mu\xi}\middle|\begin{matrix}-(m_3+m_{s,3}),-m_3\\-1,-(1+m_3)\end{matrix}\right) \times G_{3,3}^{3,2}\left(\frac{\lambda_1\lambda_2}{m_1m_2\Theta\mu}\middle|\begin{matrix}1-\rho,2,(2+m_1)\\ \varphi-\rho,(1+m_1+m_{s,1}),(1+m_1)\end{matrix}\right)d\mu \quad (22)$$

where $\Xi = \frac{\psi_2\Delta_1\Delta_3\lambda_2{}^{\rho-\varphi}\Theta^{m_1+1}}{m_2{}^{\rho}\Gamma(\varphi)\xi^{m_3+1}}$

By inverting the Meijer functions of (22) using the identity defined in [28, Eq.(9.31(2))] and converting $(1+\mu)^{-1}$ to Meijer-G function via the identity detailed in [31, Eq.(10)] and applying the identity defined in [28Eq.(7.811(5))] to the converted Meijer-G function, then the $\mathfrak{I}_2$can be further expressed as:

$$\mathfrak{I}_2 = \frac{\Xi}{ln(2)} \int_0^{\infty} G_{0,0}^{1,0}\left(\mu\middle|\begin{matrix}-\\m_1-m_3\end{matrix}\right) \times G_{2,2}^{2,1}\left(\frac{\lambda_3\xi\mu}{m_3}\middle|\begin{matrix}2,2+m_3\\1+m_3+m_{s,3},1+m_3\end{matrix}\right) \times G_{3,3}^{2,3}\left(\frac{m_1m_2\Theta\mu}{\lambda_1\lambda_2}\middle|\begin{matrix}1-\varphi+\rho,-(m_1+m_{s,1}),-m_1\\ \rho,-1,-(1+m_1)\end{matrix}\right)d\mu \quad (23)$$

By applying the integral identity defined in [32], the (23) can be solved as it given in (24) with $q_1 = 1-\varphi+\rho,-(m_1+m_{s,1}),-m_1$ and $q_2 = \rho,-1,-(1+m_1)$ where $G_{p_1,q_1:p_2,q_2:p_3,q_3}^{m_1,n_1:m_2,n_2:m_3,n_3}[.]$ is the extended generalized bivariate Meijer's G-function (EGBMGF), as defined in [33].

Thus, the system Ergodic capacity can be then expressed by putting (21) and (24) into (19) as it is detailed in (25).

$$\mathfrak{I}_2 = \frac{\Xi}{ln(2)} G_{0,0:2,2:3,3}^{1,0:2,1:2,3}\left(\begin{matrix}1+m_1-m_3\\-\end{matrix}\middle|\begin{matrix}2,2+m_3\\1+m_3+m_{s,3},1+m_3\end{matrix}\middle|\begin{matrix}q_1\\q_2\end{matrix}\middle|\frac{\lambda_3\xi}{m_3},\frac{m_1m_2\Theta\mu}{\lambda_1\lambda_2}\right) \quad (24)$$

$$\bar{C} = \frac{\Delta_3}{ln(2)\xi^{m_3+1}} G_{3,3}^{3,2}\left(\frac{\lambda_3\xi}{m_3}\middle|\begin{matrix}1+m_3, & 2, & 2+m_3\\1+m_3, & 1+m_3+m_{s,3}, & 1+m_3\end{matrix}\right) - \frac{\Xi}{ln(2)} G_{0,0:2,2:3,3}^{1,0:2,1:2,3}\left(\begin{matrix}1+m_1-m_3\\-\end{matrix}\middle|\begin{matrix}2,2+m_3\\1+m_3+m_{s,3},1+m_3\end{matrix}\middle|\begin{matrix}q_1\\q_2\end{matrix}\middle|\frac{\lambda_3\xi}{m_3},\frac{m_1m_2\Theta\mu}{\lambda_1\lambda_2}\right) \quad (25)$$

C. Average Throughput

1) Delay-Limited transmission mode

The average throughput in delay-limited transmission mode can be obtained by utilizing the outage probability at a fixed transmission rate [34]:

$$\tau_{Lim} = (1-\alpha)\tau_{Lim} \quad (26)$$

Thus, by putting (17) into (26), the average throughput under the mode can be expressed as it is given in (27).

$$\tau_{Lim} = (1-\alpha)\left\{\frac{\Delta_3}{\xi^{m_3+1}}\mu^{-(m_3+1)}G_{2,2}^{1,2}\left(\frac{m_3}{\lambda_3\mu\xi}\middle|\begin{matrix}-(m_3+m_{s,3}),-m_3\\-1,-(1+m_3)\end{matrix}\right) - \frac{\psi_2\Delta_1\Delta_3\lambda_2{}^{\rho-\varphi}\Theta^{m_1+1}}{m_2{}^{\rho}\Gamma(\varphi)\xi^{m_3+1}} \times \mu^{m_1-m_3}G_{2,2}^{1,2}\left(\frac{m_3}{\lambda_3\mu\xi}\middle|\begin{matrix}-(m_3+m_{s,3}),-m_3\\-1,-(1+m_3)\end{matrix}\right)G_{3,3}^{3,2}\left(\frac{\lambda_1\lambda_2}{m_1m_2\Theta\mu}\middle|\begin{matrix}1-\rho,2,(2+m_1)\\ \varphi-\rho,(1+m_1+m_{s,1}),(1+m_1)\end{matrix}\right)\right\}C_{th} \quad (27)$$

2) Delay-Tolerant transmission mode

The average throughput in delay-tolerant transmission mode can be determined by using the ergodic capacity at any constant rate [34]:

$$\tau_{Tol} = (1-\alpha)\bar{C} \quad (28)$$

Hence, by substituting (25) into (28), the average throughput under the mode can be expressed as it is given in (29).

$$\tau_{Tol} = (1-\alpha)\left\{\frac{\Delta_3}{ln(2)\xi^{m_3+1}} G_{3,3}^{3,2}\left(\frac{\lambda_3\xi}{m_3}\middle|\begin{matrix}1+m_3, & 2, & 2+m_3\\1+m_3, & 1+m_3+m_{s,3}, & 1+m_3\end{matrix}\right) - \frac{\Xi}{ln(2)} G_{0,0:2,2:3,3}^{1,0:2,1:2,3}\left(\begin{matrix}1+m_1-m_3\\-\end{matrix}\middle|\begin{matrix}2,2+m_3\\1+m_3+m_{s,3},1+m_3\end{matrix}\middle|\begin{matrix}q_1\\q_2\end{matrix}\middle|\frac{\lambda_3\xi}{m_3},\frac{m_1m_2\Theta\mu}{\lambda_1\lambda_2}\right)\right\} \quad (29)$$

IV. Numerical Results and Discussions

In this section, the analytical results of the derived system outage probability, Ergodic capacity and the average throughput under the delay-limited and delay-tolerant transmission modes are presented. In evaluating the system performance, the following parameters are set to be: $d_1 = d_2 = 5\,m$, $\eta = 0.75$, $\zeta_1 = \zeta_1 = 2$, $m_2 = m_{s,2} = 1$, $\sigma_D^2 = 0.5$, $\mathrm{m}_2 = 1$, $\mathrm{m}_{s,2} = 1$ and $R_{th} = 0.2bps/Hz$ unless otherwise specified in relation to [4, 21]. Hence, Monte Carlo simulations are provided to corroborate the presented analysis and these are performed by generating 10^5 independent channel realizations. In all cases, the results show that analytical results are well agreed with the simulation results which validate the correctness of the derived analytical `expressions.

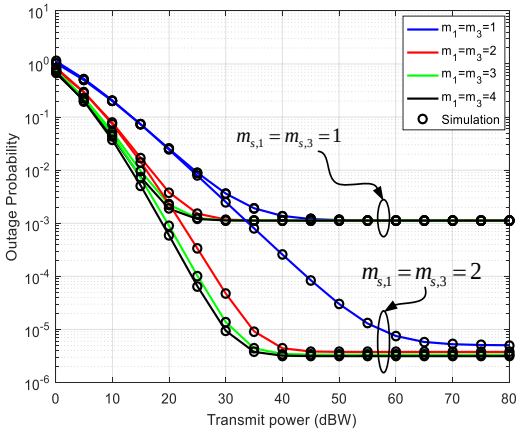

Fig. 2. Impact of fading severity and shadowing parameters of S-to-R and LSI links on the outage probability when $\mathrm{m}_2 = 2$, $\mathrm{m}_{s,2} = 1$, $\Omega_1 = \Omega_2 = 15dB$ and $\Omega_3 = -15dB$

The impact of fading severity and shadowing parameter of S-to-R and LBI links on the concerned system performance is presented in Fig. 2. It can be deduced that the outage probability decreases as the function of increasing in value of the link parameters. This is because shadowing vanishes as the $m_{s,i} \to \infty$ and also the large values of m signifies moderate fading effect which present a noticeable improvement in the outage probability of the system.

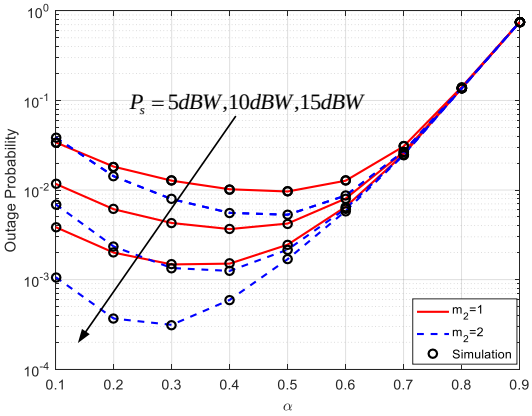

Fig. 3. Outage probability as a function of α under different values of P_s when $\Omega_1 = 25dB$, $\Omega_2 = 15dB$ and $\Omega_2 = -10dB$

The system outage performance as a function of EH time factor α under different values of source transmit power is illustrated in Fig. 3. The results show that as the transmit power increases the better the system outage probability performance. Also, it can be observed that for either small or large values of α, the higher the value of outage probability. Therefore, optimum value of α needs to be selected to achieve minimum outage probability for the system. In this case, the optimum value of α thus depends on the source transmit power as the increase in P_s leads to decrease in the values of α. Also, the results prove that the increase in the value of fading parameter on the R-to-D enhances the system outage probability.

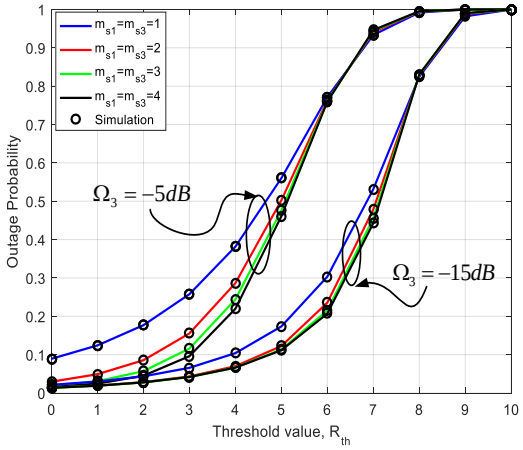

Fig. 4. Outage probability as a function of $\mathcal{R}$ under different values of Ω_3, $m_{s,1}$and $m_{s,3}$ when $P_s = 15dBW$, $\Omega_1 = 25dB$ and $\Omega_2 = 15dB$

The outage probability performance of the concerned system with respect to threshold value R_{th} under different values of Ω_3 and shadowing severity of S-to-R and LBI links is demonstrated in Fig. 4. It can be deduced that the higher the values of Ω_3, the worsen the system outage performance since large value of Ω_3 signifies high loop back interference which degrade the system performance. For every value of Ω_3, the decrease in shadowing parameter $(m_{s,i} \to \infty)$ of the considered links yields better system outage probability.

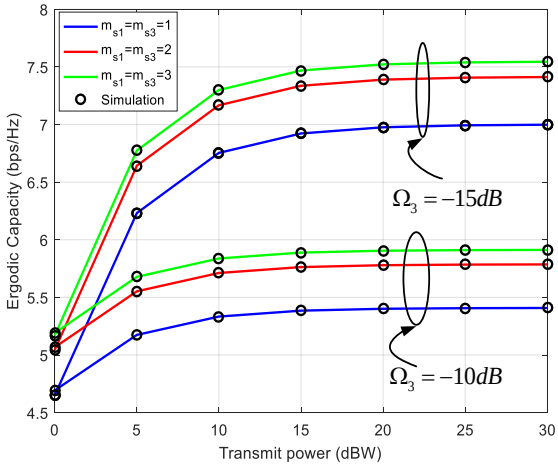

Fig. 5. Effect of shadowing parameters of S-to-R and LSI links on the system Ergodic capacity under different values of Ω_3 when, $\Omega_1 = 40dB$ and $\Omega_2 = 15dB$

The effect of shadowing parameter of S-to-R and LBI links on the system Ergodic capacity under various value of Ω_3 is presented in Fig. 5. The results clearly show that there is significant improvement in the system capacity with the decrease in value of Ω_3 since small value of Ω_3 implies a weaker residual loopback interference. Also. It can be observed that the decrease in shadowing parameter $(m_{s,i} \to \infty)$ of S-to-R and LBI links enhances the system capacity performance.

In Fig. 6, the impact of the end-to-end distance $(d = d_1 + d_2)$ on the system Ergodic capacity with respect to different values of shadowing parameter of S-to-R and LBI links is illustrated. It can be inferred from the results that the system capacity improves as the source transmit power increase and worsen with the increase in the end-to-end distance. It is noticeable that the increase in the values of shadowing effect on the S-to-R and LBI links enhances the system ergodic capacity performance.

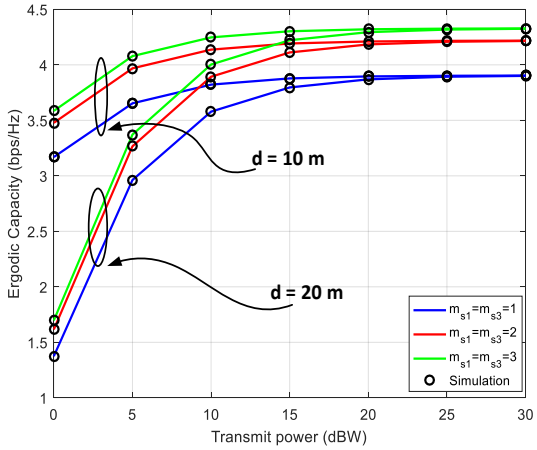

Fig. 6: Impact of link distance $(d = d_1 + d_2)$ on the system Ergodic capacity under different values of $m_{s,1}$and $m_{s,3}$when $\Omega_1 = 45dB$ and $\Omega_2 = 10dB, \Omega_3 = -5dB$

Moreover, the average throughput performance of the system under the delay-limited transmission mode as a function of the distance between the source and relay node is depicted in Fig. 7 under different values of fading severity of S-to-R and LBI links. The results show that the increase in the value of the fading parameter on the of S-to-R and LBI links offers the system better throughput performance. Also, it is noted that the increase in the distance between the source and the relay decreases the system throughput and yield poor performance at the mid-way between the source and the destination. This is because the EH reaches its peak values which significantly affect the time designated for information transmission.

In addition, the performance of the system average throughput under the delay-tolerant transmission mode as a function of the distance between the source and relay node for different values of source transmit power is presented in Fig. 8. The results depict that the increase in transmit power P_s improves the system average throughput. As the same with the Fig. 7, the increase in d_1 drastically degrade the system average throughput.

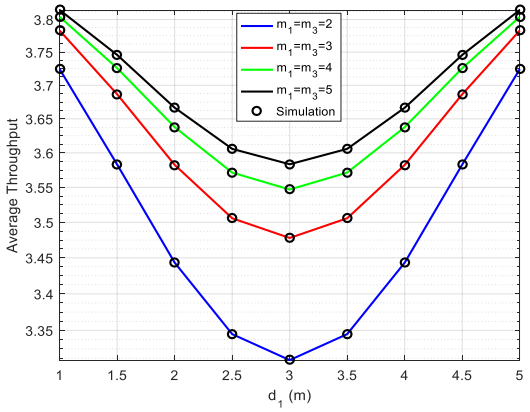

Fig. 7. Average throughput for delay-limited transmission as function of S-to-R link distance under different values of fading severity $m_1 = m_3$ when $m_2 = 2$, $m_{s,2} = 1$, $P_s = 10\ dBW$, $\Omega_1 = 35\ dB$, $\Omega_2 = 15dB$ and $\Omega_3 = -15dB$ at $R = 5\ bps/Hz$ and $d_2 = 6 - d_1$

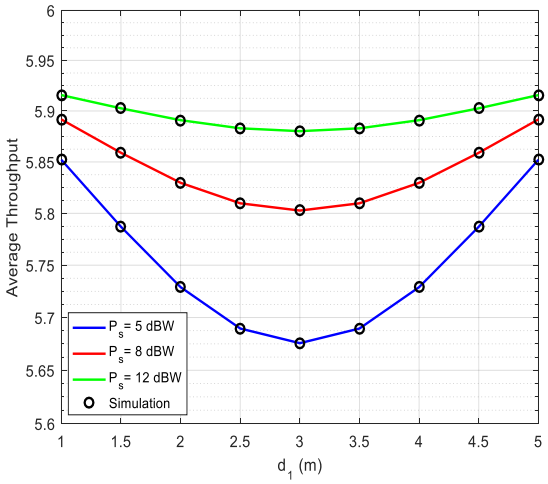

Fig. 8. Average throughput for delay-tolerant transmission as function of S-to-R link distance under different values of P_s when$d_2 = 6 - d_1$, $\Omega_1 = 35\ dB, \Omega_2 = 15dB$ and $\Omega_3 = -15dB$

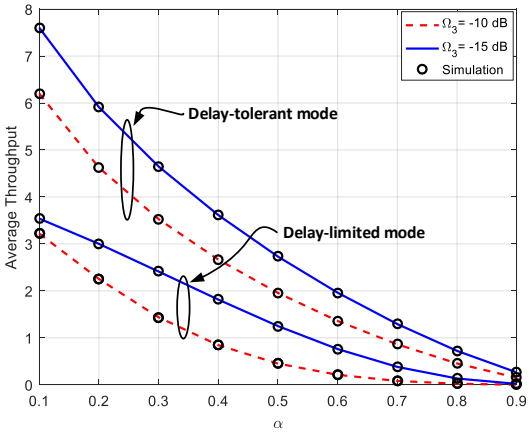

Fig. 9. Comparison between the average delay-limited and delay-tolerant transmission as function of α under different values of Ω_3 when $P_s = 15\ dBW$, $\Omega_1 = 45dB$ and $\Omega_2 = 15dB$ at $R = 4\ bps/Hz$

The average throughput performance comparison between the delay-limited and delay-tolerant

transmission mode under different values of Ω_3 is presented in Fig. 9 as a function of EH time factor α. The results depict that the average throughput of both modes is a decreasing function of α. In this case, at small value of α , the better the system throughput snice large amount of time is used for information transmission. In addition, it can be deduced that the decrease in values of Ω_3 offers the system better throughput under the two transmission modes. Also, it is observed that the delay-tolerant mode outperforms the delay-limited mode. This is because the average throughput of the delay-tolerant mode is limited by $(1-\alpha)\bar{C}$ while the delay-limited mode throughput is limited by $(1-\alpha)R_{th}$.

V. Conclusion

In this paper, the performance analysis of full-duplex wireless powered cooperative relay system over F-distribution channel is present. The concerned system analytical closed-form expressions of outage probability and Ergodic capacity are derived. Through these, the average delay-limited and average delay-tolerant throughput are obtained. The accuracy of the derived analytical expression is validated through the Monte-Carlo simulations. The results illustrated the significant impact of fading parameters on the system performance. In addition, it is noticed from the results that the increase in the values of Ω_3 significantly degrade the system outage probability and capacity.

Conflict of Interest

The authors declare no conflict of interest.

Author Contributions

Kehinde Odeyemi: Conceptualization, Methodology, Software, Formal analysis and Writing- Original draft preparation. Pius A. Owolawi: Supervision and Project administration. Kehinde Odeyemi and Pius A. Owolawi Validation, Writing- Reviewing and Editing

References

[1] M. Toka and O. Kucur, "Outage analysis of TAS/MRC in dual hop full-duplex MIMO relay networks with co-channel interferences," *AEU-International Journal of Electronics Communications*, vol. 77, pp. 82-90, 2017.

[2] T. Riihonen, S. Werner, and R. Wichman, "Hybrid full-duplex/half-duplex relaying with transmit power adaptation," *IEEE Transactions on Wireless Communications*, vol. 10, no. 9, pp. 3074-3085, 2011.

[3] D. W. K. Ng, E. S. Lo, and R. Schober, "Dynamic resource allocation in MIMO-OFDMA systems with full-duplex and hybrid relaying," *IEEE Transactions on Communications*, vol. 60, no. 5, pp. 1291-1304, 2012.

[4] G. Nauryzbayev, M. Abdallah, and K. M. Rabie, "Outage probability of the EH-Based Full-Duplex AF and DF relaying systems in $\alpha-\mu $ environment," in *Proc. IEEE 88th Vehicular Technology Conference (VTC-Fall)*, 2018, pp. 1-6.

[5] C. Li, B. Xia, and Z. Chen, "A new hybrid half-duplex/full-duplex relaying system with antenna diversity," in *Proc. IEEE 85th Vehicular Technology Conference (VTC Spring)*, 2017, pp. 1-5.

[6] M. Mohammadi, H. A. Suraweera, G. Zheng, C. Zhong, and I. Krikidis, "Full-duplex MIMO relaying powered by wireless energy transfer," in *Proc. IEEE 16th International Workshop on Signal Processing Advances in Wireless Communications (SPAWC)*, 2015, pp. 296-300.

[7] Z. Wei, X. Zhu, S. Sun, Y. Huang, A. Al-Tahmeesschi, and Y. Jiang, "Energy-efficiency of millimeter-wave full-duplex relaying systems: Challenges and solutions," *IEEE Access*, vol. 4, pp. 4848-4860, 2016.

[8] B. C. Nguyen, T. M. Hoang, and S. G. Choi, "Full-duplex relay system with energy harvesting: Outage and symbol error probabilities," in *Proc. International Conference on Advanced Technologies for Communications (ATC)*, 2018, pp. 360-365.

[9] P. A. Owolawi and K. O. Odeyemi, "On the outage performance of partial relay selection aided NOMA system with energy harvesting and outdated CSI over Non-Identical channels," *Progress in Electromagnetics Research*, vol. 95, pp. 107-117, 2019.

[10] P. N. Son and T. T. Duy, "Performance analysis of underlay cooperative cognitive full-duplex networks with energy-harvesting relay," *Computer Communications*, vol. 122, pp. 9-19, 2018.

[11] C. Zhong, H. A. Suraweera, G. Zheng, I. Krikidis, and Z. Zhang, "Wireless information and power transfer with full duplex relaying," *IEEE Transactions on Communications*, vol. 62, no. 10, pp. 3447-3461, 2014.

[12] Q. N. Le, N. T. Do, V. N. Q. Bao, and B. An, "Full-duplex distributed switch-and-stay networks with wireless energy harvesting: design and outage analysis," *EURASIP Journal on Wireless Communications Networking*, vol. 2016, no. 1, pp. 1-16, 2016.

[13] A. A. Nasir, X. Zhou, S. Durrani, and R. A. Kennedy, "Relaying protocols for wireless energy harvesting and information processing," *IEEE Transactions on Wireless Communications*, vol. 12, no. 7, pp. 3622-3636, 2013.

[14] Z. Mobini, M. Mohammadi, and C. Tellambura, "Wireless-powered full-duplex relay and friendly jamming for secure cooperative communications," *IEEE Transactions on Information Forensics Security*, vol. 14, no. 3, pp. 621-634, 2018.

[15] W. Mou, Y. Cai, W. Yang, W. Yang, X. Xu, and J. Hu, "Exploiting full duplex techniques for secure communication in SWIPT system," in *Proc. International Conference on Wireless Communications & Signal Processing (WCSP)*, 2015, pp. 1-6.

[16] M. G. Khafagy, M. S. Alouini, and S. A ïsa, "Full-duplex relay selection in cognitive underlay networks," *IEEE Transactions on Communications*, vol. 66, no. 10, pp. 4431-4443, 2018.

[17] W. Han, J. Ge, and J. Men, "Performance analysis for NOMA energy harvesting relaying networks with transmit

antenna selection and maximal-ratio combining over Nakagami-m fading," *IET Communications*, vol. 10, no. 18, pp. 2687-2693, 2016.
[18] B. C. Nguyen, T. M. Hoang, and P. T. Tran, "Performance analysis of full-duplex decode-and-forward relay system with energy harvesting over Nakagami-m fading channels," *AEU-International Journal of Electronics Communications*, vol. 98, pp. 114-122, 2019.
[19] S. Sabat, P. K. Sharma, and A. Gandhi, "Full-duplex mobile cognitive radio network under Nakagami-m fading environment," *AEU-International Journal of Electronics Communications*, vol. 109, pp. 136-145, 2019.
[20] K. M. Rabie, B. Adebisi, and M. S. Alouini, "Half-duplex and full-duplex AF and DF relaying with energy-harvesting in log-normal fading," *IEEE Transactions on Green Communications Networking*, vol. 1, no. 4, pp. 468-480, 2017.
[21] K. Rabie, B. Adebisi, G. Nauryzbayev, O. S. Badarneh, X. Li, and M. S. Alouini, "Full-duplex energy-harvesting enabled relay networks in generalized fading channels," *IEEE Wireless Communications Letters*, vol. 8, no. 2, pp. 384-387, 2018.
[22] K. Rabie, *et al.*, "On the performance of Non-Orthogonal multiple access over composite fading channels," arXiv preprint arXiv:.07860, 2020.
[23] M. Simonović, A. Cvetković, J. Manojlović, and V. Nikolić, "Outage performance evaluation of device-to-device system with energy harvesting relay," *Thermal Science*, pp. 196-196, 2020.
[24] O. S. Badarneh, D. B. da Costa, P. C. Sofotasios, S. Muhaidat, and S. L. Cotton, "On the sum of Fisher–Snedecor $\mathcal {F} $ variates and its application to Maximal-Ratio combining," *IEEE Wireless Communications Letters*, vol. 7, no. 6, pp. 966-969, 2018.
[25] S. K. Yoo, S. L. Cotton, P. C. Sofotasios, M. Matthaiou, M. Valkama, and G. K. Karagiannidis, "The Fisher–Snedecor $\mathcal {F} $ distribution: A simple and accurate composite fading model," *IEEE Communications Letters*, vol. 21, no. 7, pp. 1661-1664, 2017.
[26] S. K. Yoo, *et al.*, "A comprehensive analysis of the achievable channel capacity in $\mathcal {F} $ composite fading channels," *IEEE Access*, vol. 7, pp. 34078-34094, 2019.
[27] L. Kong and G. Kaddoum, "On physical layer security over the fisher-snedecor ${\mathcal {F}} $ wiretap fading channels," *IEEE Access*, vol. 6, pp. 39466-39472, 2018.
[28] I. Gradtejn, I. Ryik, and A. Jeffrey, *Table of Integrals, Series, and Products*, 1980.
[29] K. O. Odeyemi and P. A. Owolawi, "Relay selection in energy harvesting aided mixed RF/FSO system with transmit antenna selection over atmospheric turbulence and pointing error," *Progress in Electromagnetics Research*, vol. 97, pp. 139-150, 2019.
[30] E. Zedini, I. S. Ansari, and M. S. Alouini, "Unified performance analysis of mixed line of sight RF-FSO fixed gain dual-hop transmission systems," in *Proc. IEEE Wireless Communications and Networking Conference (WCNC)*, 2015, pp. 46-51.
[31] V. Adamchik and O. Marichev, "The algorithm for calculating integrals of hypergeometric type functions and its realization in REDUCE system," in *Proc. International Symposium on Symbolic and Algebraic Computation*, 1990, pp. 212-224.
[32] H. Lei, C. Gao, I. S. Ansari, Y. Guo, G. Pan, and K. A. Qaraqe, "On physical-layer security over SIMO generalized-$ K $ fading channels," *IEEE Transactions on Vehicular Technology*, vol. 65, no. 9, pp. 7780-7785, 2015.
[33] B. Sharma and R. Abiodun, "Generating function for generalized function of two variables," *Proceedings of the American Mathematical Society*, vol. 46, no. 1, pp. 69-72, 1974.
[34] O. S. Badarneh, D. B. Da Costa, and P. H. J. Nardelli, "Wireless-Powered communication networks with random mobility," *IEEE Access*, vol. 7, pp. 166476-166492, 2019.

Copyright © 2021 by the authors. This is an open access article distributed under the Creative Commons Attribution License (CC BY-NC-ND 4.0), which permits use, distribution and reproduction in any medium, provided that the article is properly cited, the use is non-commercial and no modifications or adaptations are made.

Kehinde Oluwasesan Odeyemi received his B.Tech. degree in Electronic Engineering from Ladoke Akintola University of Technology Ogbomosho, Nigeria, in 2008. He later obtained an M.Eng. degree in the same field from the Federal University of Technology, Akure in 2012. He received his Ph.D. degree in Electronic Engineering at the University of KwaZulu-Natal, Durban, South Africa in 2018. He joined department of Electrical and Electronic Engineering, University of Ibadan, in 2012. He has written several research articles and his research interests are in antenna design, optical wireless communications, cooperative communication, cognitive radio network, physical layer security and Green energy.

Pius Adewale Owolawi received his B.Tech. degree in Physics/Electronics from the Federal University of Technology, Akure, in 2001. He then obtained an M.Sc. and Ph.D. degrees in Electronic Engineering from the University of KwaZulu-Natal in 2006 and 2010, respectively. Presently, he is the Head of department of Computer Systems Engineering, Tshwane University of Technology, Pretoria, South Africa. He holds several industry certifications and his research interests are in the computational of Electromagnetic, modeling of radio wave propagation at high frequency, fiber optic communication, radio planning and optimization techniques and renewable energy. He has written several research articles and serves as a reviewer for many scientific journals.